Ice-slurry production for solar-ice systems using supercooling with an in-stream crystallizer

Ann-Katrin Thamm[1], Kevin Erb[1], Ignacio Gurruchaga[1], Daniel Carbonell[1,2]

[1]SPF Institut fur Solartechnik, OST – Ostschweizer Fachhochschule, Oberseestr. 10, CH-8640 Rapperswil, Switzerland
[2]DCarbo Energy Consulting S.L. 08182, Barcelona, Spain.

Abstract

Using ice slurry produced from supercooled water with an in-stream crystallizer opens a new path for solar-ice systems, increasing efficiency and reducing investment cost compared to ice-on-coil systems. Power needs are decoupled from the stored energy since the heat exchangers are not evenly distributed in the ice storage vessel but directly placed as the heat pump evaporator, which depends on the heat pump capacity and not on the ice storage volume. The novel ice storage design can serve as a heat source for a heat pump, where its evaporator is used to supercool water below 0 °C, or for refrigeration. The supercooled water at a temperature around −2 °C, maintained in a meta-stable liquid state, is triggered to nucleate in an in-stream crystallizer. The current design of the ice crystallizer allows for continuous operation of the system and scalability. Experimental results obtained with a gasketed plate heat exchanger used to supercool water and an in-stream crystallizer operated at a power of up to 6.5 kW are presented.

Keywords: supercooling, ice slurry, solar-ice, ice storage, in-stream, crystallizer

1. Introduction

In the near future the European energy system will include a lot of heat pumps to supply residential buildings with heating and cooling (Lyons, et al., 2023). However, which heat sources these heat pumps will use will depend on many factors such as regulations and social acceptance including the noise of fans for Air Source Heat Pumps (ASHP) as well as aesthetics, ground water regulations, wastewater availability, etc. Thus, to cover many local and regional needs, several heat sources for heat pumps need to be considered. Solar-ice systems, combining solar thermal collectors, a heat pump and an ice storage solution, are promising candidates for supplying heating demands to buildings in heating dominated climates with enough solar radiation in winter. The ice storage can serve as a heat source for the heat pump in periods of insufficient amount of direct heat from the solar thermal collectors, e.g. during night or days with low irradiation. During times of high irradiation, excess heat, not required for the heat pump, can be used to regenerate the ice storage and can also provide heat for domestic hot water or space heating (Carbonell, et al., 2016). In this context, a solar-ice systems is usually considered as an alternative to Ground Source Heat Pumps (GSHP) since it can achieve the same efficiency with the additional benefit of not needing to drill boreholes. When compared to GSHP, a solar-ice system offers an often-missed benefit: it does not need further regeneration in the long term since it regenerates on a yearly basis.

Most of the ice storages installed in Europe, used in solar-ice systems or for refrigeration, are based on coil heat exchangers and are known as ice-on-coil storages (Nelson, et al., 1996). An anti-freeze solution is circulating in tubes embedded into the storage-vessel, serving as heat exchanger. Ice is formed on the outer surface of the tubes, acting as a growing insulating layer due to the low thermal conductivity of ice, limiting the amount of ice per unit surface area of the heat exchanger (Carbonell, et al., 2022). Thus, the tubes need to be distributed along the storage volume coupling power and capacity needs. Consequently, the cost for the heat exchanger scales with capacity of the ice storage.

In order to keep the heat transfer area free of ice, two concepts have been proposed earlier at our institute: the thermal de-icing approach (Philippen, et al., 2012; Carbonell, et al., 2015) and an ice slurry concept (Carbonell, et al., 2020). While the thermal de-icing concept still needs an indeed reduced number of heat

10.18086/eurosun.2024.08.04 Available at http://proceedings.ises.org

exchangers in the storage, the slurry concept decouples ice generation and storage volume avoiding continuous ice growth on the heat exchanger surface, while the produced slurry remains pumpable (Kauffeld, et al., 2005). Possibilities to avoid that ice grows at the heat exchanger surface completely, are based on slurry concepts using direct contact evaporation with a refrigerant (Wijeysundera, et al., 2004), water vacuum freezing (Honke, et al., 2015) or supercooling (Tanino & Kozawa, 2001). The second possibility to keep the surface free of ice is to continuously remove it from the surface, e.g. by fluidized beds (Pronk, et al., 2003), supercooled water jets (Mouneer, et al., 2010), blowing compressed air (Zhang, et al., 2008) or using scrapers (Stamatiou, et al., 2005). The latter is the most common method in commercial ice slurry systems nowadays and uses mechanically scraped-surface heat exchangers, where ice is formed on a cold surface and is then removed continuously by a rotating mechanical arm that scrapes ice from a cylindrical barrel. The scraper design, having a mechanical component, requires high operation and maintenance cost, and has limited potential for scale up due to the mechanical constrains of the rotating-scraping arm.

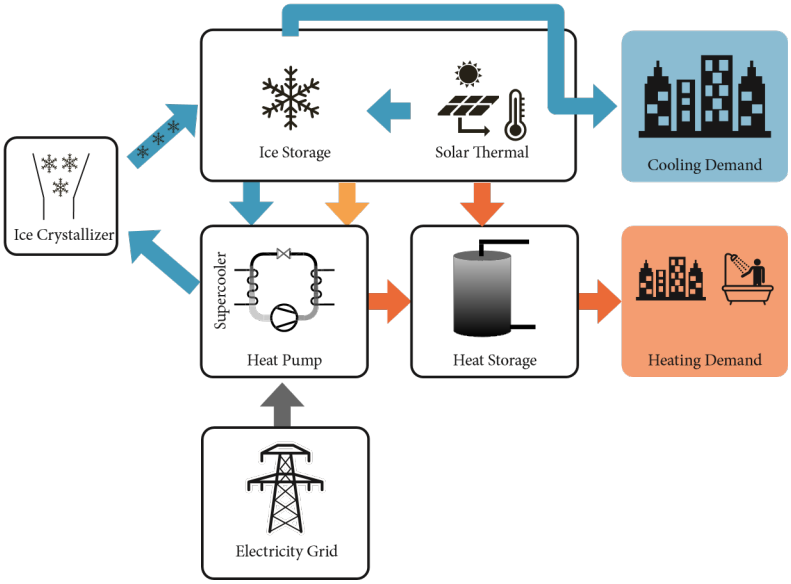

Figure 1: General scheme of a solar ice-slurry system using the supercooling approach.

To reduce installation and maintenance cost as well as improving energy efficiency and reliability of the ice storage implemented in a solar-ice system, a passive concept for ice slurry production based on the supercooling method (see Fig. 1) was proposed earlier in Carbonell et al. (2020). In Gurruchaga et al. (2023a) the investment costs of solar-ice slurry systems were estimated to be between 8 % to 11 % lower than the reference ice-on-coil system in Bilbao and between 14 % to 17 % lower in Zurich. The heat generation costs in ct/kWh were between 7 % to 12 % lower for the slurry version. Moreover, the system is conceived such that the used heat exchanger is always free of ice and thus a higher efficiency compared to the ice-on-coil method for large ice fractions can be reached. Arenas-Larranaga et al. (2024) numerically demonstrated the system performance of such solar-ice slurry systems for several European climates and two multi-family buildings using natural refrigerant heat pumps with supercooling evaporators.

Besides numerical simulations, a hardware-in-the-loop Concise Cycle Test (Haberl, et al., 2022) was used to validate in the laboratory the autonomous operation of a solar-ice slurry system and assessed its performance during a whole year using an accelerated system test methodology (Gurruchaga, et al., 2023b). Specifically, a 10 kW CO_2 heat pump with a coated supercooler-evaporator developed in Carbonell et al. (2022) was tested with a complete system including hydraulics, thermal storages, electrical battery, inverter and an autonomous control. To provide the appropriate dynamic boundary conditions for the system, the solar thermal collectors, PV and building demands were simulated and emulated. The system was working continuously efficiently and reliable for two consecutive weeks. However, key parts of the ice slurry system i.e., the in-stream ice crystallizer and storage vessel, were simulated and emulated due to lack of reliable devices at the appropriate

power needs. In the current work, a working and scalable crystallizer is demonstrated experimentally in the laboratory with a power of 6.5 kW as one of the missing pieces of the complete solar ice-slurry system.

1.1. Ice slurry generation using supercooling approach

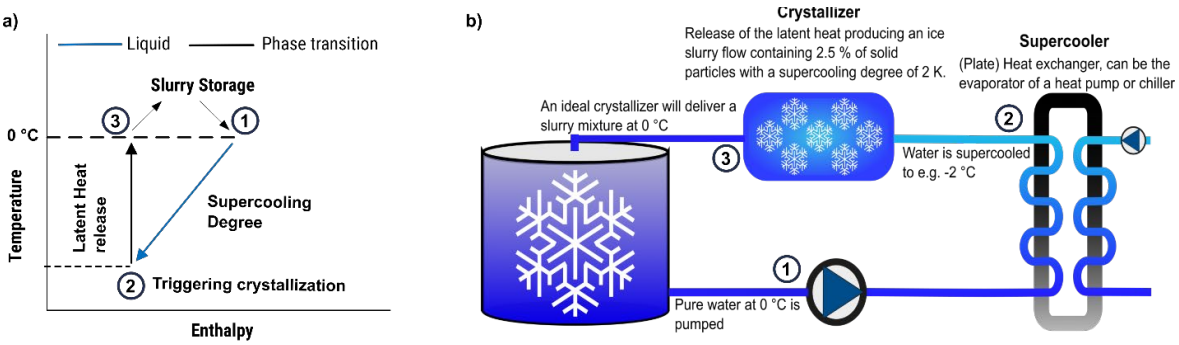

Figure 2: a) Temperature as a function of enthalpy using supercooling for ice slurry production. b) Conceptual visualisation of the supercooling concept. a) and b) are linked via points 1 to 3: Pure liquid water at a temperature of 0 °C (1), is pumped into the supercooler, where it is supercooled and remains in a metastable liquid state (2). The supercooled water is crystallized in an in-stream crystallizer, releasing sensible heat into latent heat, and is pumped into the storage vessel as slurry (3).

The supercooling concept with an in-stream crystallizer to produce ice slurry is visualised in Fig. 2 b), while Fig. 2 a) shows the temperature as a function of system enthalpy during the process. Both are linked via the indicated state points 1 to 3. Liquid water at a temperature of 0 °C is pumped from the storage vessel (state point 1) into a standard plate heat exchanger - the supercooler - where it undergoes supercooling, e.g. to a temperature of −2 °C and stays in a metastable liquid phase (state point 2). The supercooling degree is defined as the difference between the melting temperature T_m and the meta-stable liquid water temperature T_{wat} in Kelvin: $\Delta T_{sup}=T_m-T_{wat} > 0$ K. After the supercooler, the stored sensible heat is transformed into latent heat triggered by the nucleation mechanism placed in-stream inside the crystallizer. The conversion from sensible to latent heat leads to a mass ice fraction on the fluid flow of approximately 2.5 % at a supercooling degree of 2 K. Thus, the slurry will leave the crystallizer with a temperature of 0 °C (state point 3), which prevents the piping system of being clogged as the freezing potential has been exhausted, i.e. all sensible heat is converted into latent heat during the phase change from supercooled water to ice inside the crystallizer. After the in-stream crystallizer, the slurry is pumped into the storage vessel. For the system to work, phase separation between solid and liquid must be guaranteed in the storage vessel, as no ice crystals should be pumped into the supercooler, where they would cause a freezing event immediately. For this, the relatively large density difference between ice and water is beneficial. On top of that, the storage vessel is equipped with some internal design to guarantee proper phase separation inside the vessel.

Due to the instability of the supercooling method, attributed to the fact that ice nucleation in supercooled water has a stochastic nature (Kauffeld, et al., 2005), not a single system using the supercooling approach has been installed in Europe nowadays, contrary to Japan, where several companies made use of the method in air-conditioning (Tanino & Kozawa, 2001; Kozawa, et al., 2005; Kurihara & Kawashima, 2001) more than 20 years ago. For the concept to work, three main challenges need to be solved: i) reliable supercooling of the water needs to be achieved in the heat exchanger and maintained downstream of it before entering the crystallizer; ii) the supercooled water needs to be crystallized in a defined location, in our case in the in-stream crystallizer, without causing blockage in the hydraulics downstream and avoiding upstream ice propagation into the supercooler and iii) produced ice slurry needs to be stored in the vessel with a high mass ice fraction avoiding even small ice particles from being pumped into the supercooler where they would cause crystallization.

While challenge i) has been a research topic in Europe since years (Saito & Okawa, 1994; Faucheux, et al., 2006; Bédécarrats, et al., 2010; Ernst & Kauffeld, 2016) without finding a working scalable solution, Japanese companies seem to use the supercooling approach since the beginning of the 21st century (Nagato, 2001; Kozawa, et al., 2005). However, public literature lacks giving details about the used supercooler and their stability. Just recently, Carbonell et al. (2022) demonstrated the possibility to use very compact coated brazed

plate heat exchangers as supercoolers for residential heat pumps. The ones with icephobic coatings improved the supercooling degree with respect to the non-coated reference one and reached in average supercooling degrees in the range of 3 K to 4 K for water mass flow rates of 1000 kg/h.

The efficient and reliable generation of ice slurry (challenge ii) was identified as one of the “last unravelled mysteries” by Kauffeld & Gund (2019). Successful release of supercooling potential ready for application in the kW to MW scale is - to our knowledge - only reported from researches in Japan: Tanino & Kozawa (2001) and Mito et al. (2001) proposed a free-falling stream of supercooled water into the ice storage, initiating nucleation through collision with a surface. The same researchers reported about a crystallizer where the supercooled fluid was continuously bombarded with ultrasonic waves to trigger nucleation and to prevent ice from adhering to walls (Tanino, et al., 2000). Upstream ice propagation can be avoided by using a warm laminar flow at the inside of the pipe wall according to them (Mito, et al., 2002).

In the following, we propose a solution for reliable slurry generation from supercooled water with the design of a scalable “in-stream-crystallizer”, operated at a power of 6.5 kW for almost 3 h, using an average supercooling degree of 1.75 K at a mass flow rate of 3200 kg/h. The proper separation of ice and water in the slurry storage vessel, challenge iii), will be addressed in future research work and is currently solved by using two storage vessels connected in series, one is filled with the produced slurry, and the water for the supercooler is sucked from the second storage which is free of ice for longer time periods.

2. Material and Methods

The constructed experimental set-up is described in section 2.1, followed by a short description about the tools for experimental control and data acquisition in section 2.2. Next, the test procedure to evaluate the reachable supercooling degree of heat exchangers is identified in section 2.3 and last, the development of the crystallizer used for slurry generation is explained in section 2.4.

2.1. Experimental Set-up

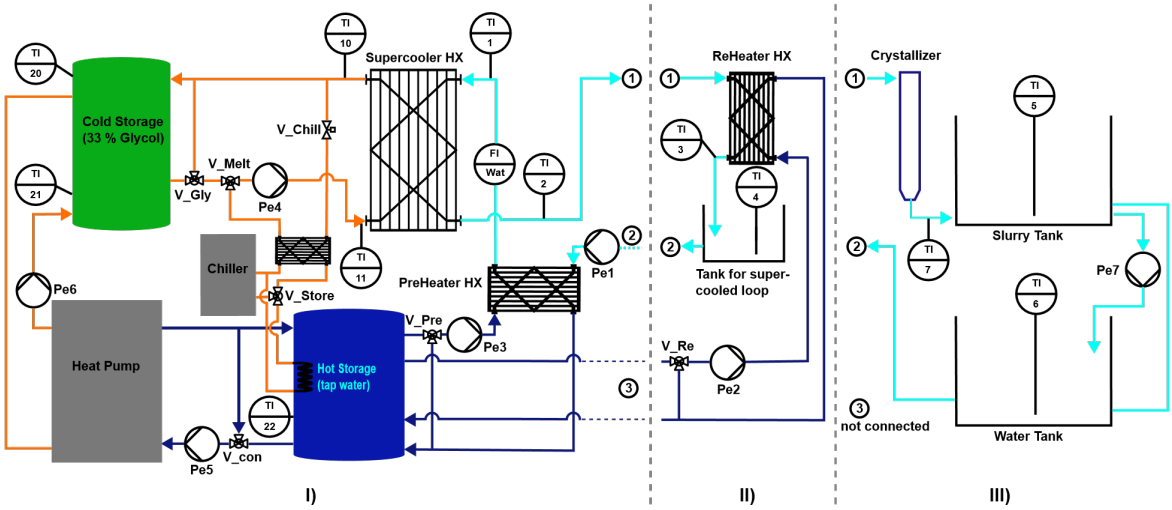

Figure 3: Schematic diagram of the experimental set-up, orange loop: glycol, cyan: supercooled loop, dark blue: tap water. I) Shared components for both supercooler and crystallizer testing. II) components for supercooler testing plugged into I) on ports 1, 2 and 3 (loop III not used). III) Components for crystallizer testing, plugged into I) via 1 and 2, 3 not connected (loop II not used).

The developed set-up (see Fig. 3) can be used for two types of experiments: the *supercooler testing* (loop part I and II) aiming at the evaluation of reachable supercooling temperatures for different mass flow rates without producing ice slurry and the *crystallizer development* testing (loop part I and III) for producing the ice slurry. Loop part I) shows the shared loop for supercooler and crystallizer testing: a heat pump operates between the hot storage (blue in Fig. 3), filled with tap water, and cold storage (green), filled with 33 % Glycol. The temperature in the cold storage (TI20 and TI21) is the control temperature for the heat pump to turn on and charge the glycol storage to the desired negative temperature. Cold glycol from the cold storage is pumped into

the supercooler, controlling TI11 (T_{GlyIn}) with Pe4 and the mixing valve V_{Gly}. If ice in the supercooler needs to be melted, hot glycol, supplied from the chiller, and connected with V_{melt} and V_{ChilI}, pumped with Pe4, can be used. In both type of experiments, the water in the supercooled loop (cyan in Fig. 3) is pumped (Pe1) from the storage into the PreHeater, a brazed plate heat exchanger used to control the inlet temperature TI1 (T_{WatIn}) of the supercooler. The hot side of the PreHeater is connected to the hot storage and the temperature can be controlled with Pe3 and V_{Pre}. The mass flow rate in the supercooled loop is measured with a Coriolis mass flow meter (Fl Wat). Pumped water is supercooled in the supercooler to a temperature TI2 (T_{WatOut}) and, depending on the type of the experiment, entering into the ReHeater for supercooler tests (loop part II) or into the crystallizer (loop part III) for controlled release of supercooling potential.

During supercooler tests, the supercooled water, in a metastable liquid state, leaving the supercooler is directly pumped into the ReHeater (see Fig. 3 part II) with only ≈ 300 mm of pipe in between the two heat exchangers. In the ReHeater the supercooled water is reheated to a temperature of 0°C, measured with temperature sensor TI3 (T_{Reheat}) and controlled by Pe2 and V_{Re}, supplied with water from the hot storage. This guarantees that no blockage of the piping system occurs before entering the storage vessel and avoids supercooling of the storage vessel content. During supercooler tests, a small storage vessel with a maximum capacity of 110 l allows for fast heating and cooling of the water in the supercooled loop.

For experimental analysis of the crystallizer, a device to release the supercooling potential in a controlled manner in a determined place, called in-stream crystallizer, is mounted after the supercooler instead of the ReHeater (see Fig. 3 part III). There, nucleation is triggered on the supercooled water forming ice slurry with a temperature of 0 °C, consisting of ice particles and liquid water with a solid mass content on the mass flow rate of less than 3 %. The produced slurry leaves the crystallizer and is fed into one of the two 1m^3 storage vessels, which are connected in series, while the ice-free water being pumped (Pe1) into the supercooler is sucked from the “ice-free” storage. Level compensation between the two storage vessels is guaranteed by a direct connection and a pump (Pe7).

2.2. Experimental control, measurements and calculation of power

The experimental control, including data acquisition, is realized using a CompactDAQ from National Instruments (NI) that establishes the communication between the computer with the in-house programmed LabView GUI and the I/O hardware modules. Used I/O modules are digital or analog modules from Wago with two to four channels each, used to control valves, pumps, heat pump and chiller. Signals from the PT100 temperature sensors, immersed into the flow, are received by 8-channel temperature input modules from NI with a precision of ± 0.03 K. During supercooler tests, the immersed temperature sensor TI2, measuring the outlet water temperature of the supercooler, is replaced by a calibrated PT100 surface sensor attached to the outlet stainless steel fitting of the supercooler to avoid obstacles in the supercooled flow. Calibration was done according to the procedure described earlier (see Carbonell et al. (2022)), but linear fit could be realized in a wider temperature range from 0.4 °C to −4 °C. The mass flow rate in the supercooled loop is measured with a Coriolis mass flow meter (precision of ± 0.15 %). Software detects freezing events, which block the hydraulic system, by a change in the mass flow rate and stops the test run, i.e. turns off pumps Pe1, Pe2, Pe3 and Pe4 as well as chiller and closes valves, in case of a blockage to avoid damage to components and allows for automated deicing of components. The supercooling power, i.e. the capacity stored in the supercooled water as sensible heat, which is converted into latent heat by inducing nucleation, can be calculated from the (indirect) measured quantities, supercooling degree, ΔT_{sup} in K, the mass flow rate of the supercooled water $\dot{m}$ in kg/h and using the specific heat of water c_P in J/(kg K) as:

$$P = \frac{Q}{t} = \frac{\dot{m} \cdot c_p \cdot \Delta T_{sup}}{t} \qquad \text{(Eq. 1)}$$

2.3. Supercooler Test Procedure

A commercial gasketed plate heat exchanger, called supercooler, with stainless steel plates is tested using part I and II of the set-up presented in Fig. 3. The water in the storage of the supercooled loop (filled with ≈ 80 l of water) is cooled down to a temperature between 0 °C and 0.1 °C. After, the test is started by keeping the glycol temperature T_{GlyIn} in the inlet of the supercooler constant at −0.4 °C for 15 min, resulting in a water

outlet temperature T_{WatOut} of approx. −0.1 °C. Next, the temperature of the glycol is decreased in steps of 0.2 K per 0.5 min. Consequently, the water outlet temperature is following the decrease in temperature. T_{GlyIn} is decreased until a "freezing" event is detected by the control program. This is achieved by monitoring the pump power required to establish the desired mass flow rate in the hydraulic system (water side): a freezing event causes an increase in the required pump power to keep the mass flow rate stable due to the increase of resistance in the hydraulic system. When the program detects a freezing event, the test is stopped and the last measured supercooling degree is taken as the achieved one for this test run. Deicing of the heat exchanger is realized by heating up the glycol flow causing a melting of the ice on the water side after some time. The water in the supercooled loop (including the water in the storage) is heated to 8 °C and a new test run can be started. During the test run the supercooled water is heated up to $T_{ReHeat} \approx 0.1$ °C after the supercooler to prevent a supercooling of the storage; the water temperature at the inlet of the supercooler T_{WatIn} is kept constant at ≈ 0.4 °C with the PreHeater during the whole test run to provide stable conditions. The achievable supercooling degree is measured 15 times for each of the water mass flow rates of 2000 kg/h, 2500 kg/h and 3000 kg/h.

To obtain comparable results the supercooled loop needs to be degassed before starting the test sequence as air bubbles present in the piping system are known to act as nucleating agents and thus to cause freezing events from previous experiments. The transparent piping system allows to detect air bubbles by eye with sufficient illumination. For every new test campaign, i.e. when a heat exchanger is replaced, fresh water at room temperature is filled into the system and the pump is started. At high pump speeds the flow is strong enough to carry away most of the air in the system. As the ability of water to absorb air is higher at lower temperatures, the water inside the supercooled loop is heated to 40 °C and constantly pumped through the loop for one night (12 hours). During this time air gets released from the water and accumulates into the open storage vessel. After roughly 12 h the water is cooled to room temperature. Repeated on/off sequences of the pump from 0 % to 100 % pump power are executed to carry away air accumulated inside dead zones of the loop. This process is supported by a valve mounted at the end of the inlet pipe (immersed into the water storage) that can be opened and closed while the pump is running, assisting the removal of air. The procedure is repeated until no air bubbles are visible in the pipes and at the inlet of the storage. Another visual check for air bubbles is done after cooling the water in the supercooled loop to 10 °C. If no air is visible, the system is ready for the supercooler tests under stable conditions.

2.4. Crystallizer Development and Test Procedure

Supercooled water, free of ice, is entering a vertically mounted in-stream crystallizer (Fig. 3 loop part III), made from transparent PVC-U, at the top of it, through a tangential inlet with reduced pipe diameter to accelerate the flow velocity (see Fig. 4 A and E). This serves as a barrier for growing ice crystals at the pipe wall upstream, into the direction of the supercooler as the force of the water on ice particles growing at the pipe wall is increased. Initially, crystallization is triggered via ultrasonic transducers attached to the external wall of the in-stream crystallizer but are turned off as soon as first ice nuclei exist inside the crystallizer. Afterwards, the nucleation process is self-sustaining due to the adhesion of very small ice crystals to upper part of the crystallizer pipe wall; ice crystals are flushed away from the wall as soon as the resistance to the water is larger as the adhesion to the wall. The dimensions of the crystallizer are such that the whole amount of stored sensible heat at a supercooling degree of 2 K and a mass flow rate of 3200 kg/h is transformed into latent heat inside the crystallizer. To ensure this was the case, pretests with an open crystallizer end, fed directly into the storage vessel, allowed to insert a temperature sensor (PT100) from the bottom to measure the slurry temperature at various positions with the aim to determine the necessary length of the device. Due to the tangential inlet, a swirl motion is introduced in the fluid flow (see Fig. 4 A), which is beneficial for mixing of ice and supercooled water and therefore the release of supercooling is further enhanced (compared to a pure axial flow). Furthermore, the possibility to use a reduction piece at the outlet of the in-stream crystallizer is strongly related to the structure of the produced ice crystals. If they agglomerate to big ice chunks inside the crystallizer, it will be more difficult for them to enter and go through the reduction. To avoid the agglomeration a higher rotational velocity component is preferable limiting the maximal diameter of the in-stream crystallizer. The outlet reduction piece is essential for being able to mount the crystallizer at any place after the supercooler

- potentially far away from the storage vessel, as the produced ice slurry can then easily be transported through a piping system consisting of various elbow pieces and pipe sections.

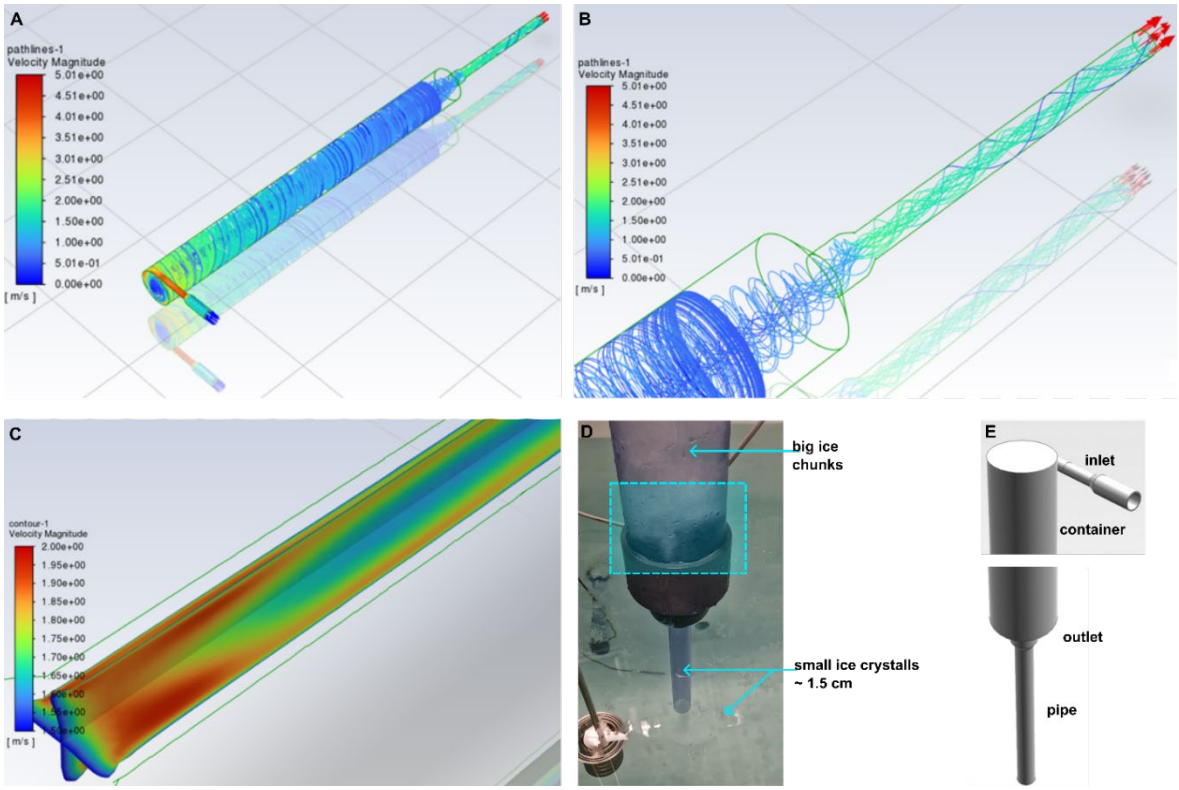

Figure 4: A: CFD simulation of a single-phase fluid (water) inside the crystallizer, showing a velocity profile of the flow (velocities given according to color bar). B: Zoom to the outlet region. C: Velocity profile in the pipe after outlet reduction, showing a fast stabilizing of the flow velocities inside the pipe. D: Photograph of the crystallizer with mounted outlet reduction and pipe, slurry fed into the storage. The cyan marked area is the area of suction effect causing a trenching of the ice crystals into smaller particles. E: CAD drawing of the crystallizer showing inlet, main crystallizer pipe, outlet and pipe.

A three-dimensional steady-state monophasic CFD model was developed to analyse the flow behaviour in the in-stream crystallizer and helped to understand the ice-slurry biphasic flow behaviour (despite the single-phase simplification) inside the crystallizer due to reduced ice content (less than 3 %). The reduction piece mounted to the outlet of the in-stream crystallizer causes a region of suction effect just above the outlet reduction and an acceleration of the fluid in this region (see Fig. 4 B). Bigger ice chunks, produced inside the in-stream crystallizer, are trenched into smaller particles in the region just above the outlet reduction (see Fig. 4 D) because of the acceleration of the flow and the arising suction. In addition, CFD simulations gave insight into the flow stabilization after the reduction piece at the outlet (see Fig. 4 C): the simulation shows that the flow inside the pipe, mounted after the reduction, is stabilizing within the first centimetres of the thin pipe, i.e. the velocity profile does not change over length of the pipe. To be able to freely mount the crystallizer in the set-up, a 90° elbow was mounted below the outlet reduction guiding the flow from vertical into horizontal direction and feeding it into one of the two installed 1 m^3 storage vessels. To fulfil all the above-described requirements the crystallizer was built step by step: first, it was tested with an open end mounted into the storage vessel. Second, the reduction piece was mounted and tested into the storage vessel. Third, the thin pipe was mounted into the reduction and cut to the appropriate length as described above and tested in the vessel. Forth, the elbow was mounted and tested into the vessel. Fifth, the crystallizer was removed from the storage vessel and mounted into the piping system.

For testing the crystallizer, the water enters the supercooler with a temperature between 0.5 °C to 1 °C and is supercooled to a stable temperature between −1.6 °C to −2.0 °C at a constant water mass flow rate (kept constant by the control program by adjusting the power of the pump). The PreHeating of the water before entering the supercooler enables stability under a broad range of working conditions melting potentially contained ice particles in the water flow. After the supercooler, the water releases its latent potential in the

crystallizer forming a slurry. Initial nucleation is triggered by ultrasonic waves at 50 kHz emitted from two to four ultrasonic transducers operated at a power of 25 W each. They are mounted to the outside of the crystallizer and the ultrasonic signal is applied for some seconds until first crystals are visible inside the crystallizer. The generated slurry is pumped though some pipes and is introduced into the storage vessel through an inlet mounted to one of the sidewalls and directed onto the center of the bottom of the storage. The feeding towards the bottom causes a wide spreading of the ice crystals, as they hit the bottom with a high velocity (1.5 m/s), before the crystals are rising by buoyancy to the highest reachable free space inside the storage vessel, unoccupied with ice yet. A crystallizer test run is considered successful if no blockage occurred in the system and if the production of slurry needs to be stopped due to a full storage, which is visible in the measurement data of the pump power and the mass flow rate (see Figure 6 B).

3. Results and Discussion

First, experimental results quantifying the supercooling degrees achieved for different water mass flow rates between 2000 kg/h to 3000 kg/h in gasketed heat exchangers are presented in section 3.1. Second, temperature and mass flow rate measurements for a successful crystallizer test with a power of 6.5 kW are shown and discussed in section 3.2.

3.1. Supercooler Test Results

Fig. 5 A) shows temperature measurements of a single test run at a mass flow rate of 2500 kg/h where the temperature of the glycol T_{GlyIn} in the supercooler (blue line) was decreased in steps of 0.2 K per 0.5 min. Water is entering into the supercooler at a temperature of 0.4 °C (T_{WatIn}, pink line). The green line is the temperature of the supercooled water leaving the supercooler T_{WaOut}, which is reheated in the ReHeater to 0 °C (T_{Reheat}, brown line). The lowest reached supercooling temperature in this test was −5.0 °C and is one of the points in Fig. 5 B) as indicated with the arrow. Fig. 5 B) summarizes results for supercooling tests performed with the supercooler and with water mass flow rates of 2000 kg/h (red), 2500 kg/h (green) and 3000 kg/h (blue). The data points correspond to the achieved supercooling temperature of single test runs, as shown in Fig. 5 A), with the average value for each mass flow rate given as the height of the corresponding bars.

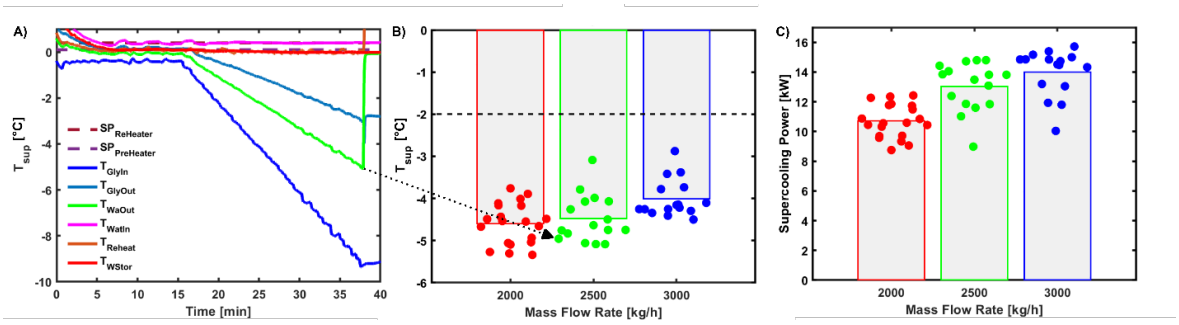

Figure 5: A) Single supercooler test-run at a water mass flow rate of 2500 kg/h with the decrease of the glycol temperature (blue line) in steps of 0.2 K per 0.5 min. The minimum supercooling temperature, which is measured at the outlet of the supercooler (T_{WaOut}, green line) is one of the points in the bar plot (B) summarizing the reached supercooling temperatures for the three evaluated different mass flow rates: 2000 kg/h = red, 2500 kg/h = green, 3000 kg/h = blue. Each point corresponds to the achieved supercooling temperature of a single test run. The bar heights give the average supercooling temperature achieved per mass flow rate. C) Comparison of corresponding supercooling power for each measurement run for water mass flow rates of 2000 kg/h, 2500 kg/h and 3000 kg/h. Each point corresponds to the power for the achieved supercooling temperature of a single test run. The bar heights give the average power achieved per mass flow rate.

The average supercooling temperature decreased from 4.6 °C ± 0.5 °C at a mass flow rate of 2000 kg/h to 4 °C ± 0.4 °C at a mass flow rate of 3000 kg/h. The spread between the highest and the lowest supercooling temperature for the same mass flow rate is 1.6 K for the mass flow rates of 2000 kg/h and 3000 kg/h, while it is 2 K for the mass flow rate of 2500 kg/h and is attributed to the stochastic nature of the freezing of supercooled water. All freezing events were detected for supercooling temperatures smaller than −2.9 °C. Despite the accelerated testing methodology used here is not the same than in our previous work (Carbonell, et al., 2022)

and results cannot be compared one to one, current results show that with large enough heat exchanger surfaces we can operate reliable at a reasonable supercooling temperature of −2 °C (dashed horizontal line in Fig. 5 B) without using icephobic coatings, provided the water quality is high and remains constant. However, the influence of water quality has not been assessed properly and will be topic of future research.

Fig. 5 C) shows the corresponding supercooling power delivered in the supercoolers from the tests of Fig. 5 B), calculated according to Eq. 1. For a mass flow rate of 3000 kg/h, an average supercooling power of 14 kW was reached.

3.2. Crystallizer Results

Temperature measurements of a successful test-run of the crystallizer with a supercooling power of 6.5 kW, operated for 3 h, at a mass flow rate of 3200 kg/h are shown in Fig. 6 A). Water was entering into the supercooler at a temperature of 1.0°C (T_{WatIn}, red line) and was supercooled to (in average) −1.75 °C (T_{WaOut}, blue line) using glycol at an average temperature of −4.5 °C (T_{GlyIn}, orange line). Slurry was continuously produced inside the crystallizer (see Figure 7 A) from the point marked with the black dashed line in Fig. 6 A) when nucleation was triggered by applying ultrasonic waves from the transducers for some seconds. The temperature of the storage filled with slurry was around 0 °C (T_{WStor}, yellow line) during the whole test, while the storage temperature of the second storage connected in series and free of ice was around 0.25 °C (upper = green, $T_{WatTank4}$; lower = purple, $T_{WatTank5}$). Fluctuations of the glycol temperature around the set-point of −4.5 °C are clearly visible in the data and are a result of the experimental control, as the glycol temperature in the inlet of the supercooler is controlled by a mixing valve (V_{Gly} in Fig. 3) with a PID-controller, determining the ratio of the glycol extracted from the cold storage into the glycol loop.

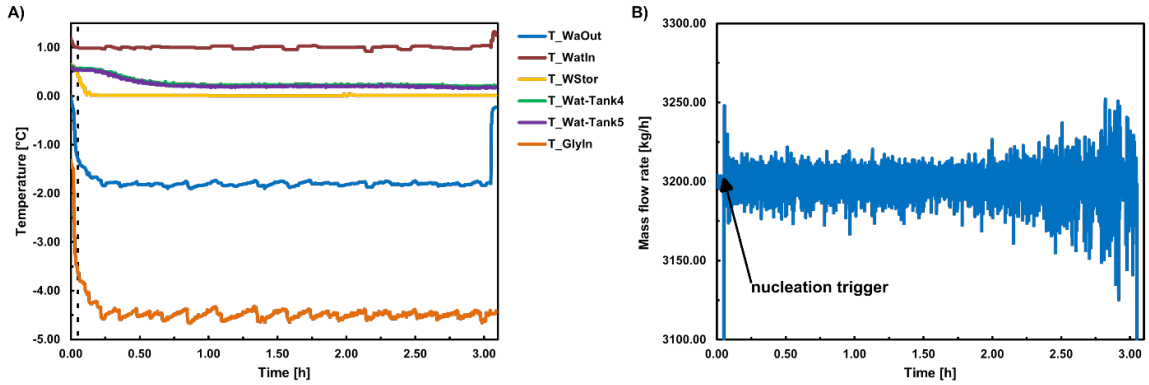

Figure 6: A) Measured temperature data for a successful 3 h test run at an average supercooling temperature of −1.75 °C (blue line, T_{WaOut}). The black dashed line marks initial triggering of nucleation by ultrasonic waves. Water is pre-heated to 1.0 °C before entering the supercooler (red line, T_{WatIn}). The temperature in the storage vessel filled with slurry is very close to zero during the whole test run (yellow line, T_{WStor}). The temperature in the second storage vessel (ice-free) is around 0.25 °C during the test run (upper = green, $T_{WatTank4}$; lower = purple, $T_{WatTank5}$). B) Mass flow rate with an average of 3200 kg/h for the same test run. The arrow marks the initial nucleation by ultrasound, the black dashed line marks the beginning of strong fluctuations in the mass flow rate due to high ice content in the storage vessel.

The PID controller is tuned as good as possible, while the temperature of the glycol in the storage is also dependent on the status of the heat pump (running or off). The fluctuations of the glycol temperature have an influence on the supercooling temperature in the water loop, which can be seen in the fluctuations of T_{WaOut} signal (blue line). However, the amplitude of fluctuations in the supercooled water temperature is less distinct as in the glycol temperature. Nevertheless, the fluctuations in the supply temperature (glycol) and the so caused fluctuations in the supercooling temperature are not causing any issue in the slurry production inside the crystallizer indicating a sign for the robustness of the device.

Fig. 6 B) shows the signal of the mass flow rate measurement, where the black arrow marks the triggering of initial nucleation by ultrasound. Starting at a time of ≈ 2.1 h, indicated with the black dashed line, the mass flow rate starts to fluctuate stronger which can be attributed to the filling of the $1m^3$ ice storage with ice particles. The produced ice particles introduced into the vessel towards a central spot at the bottom (see Fig. 7 B) are distributed almost randomly inside the storage vessel, with some asymmetry caused by the suction

of the pump. With time, the storage vessel is filled with ice from top to bottom, as introduced ice particles rise due to buoyant forces. When most of the vessel is filled with ice, new ice particles start to accumulate close to the slurry-inlet into the storage as no space is left for ice particles to move around. Thus, pressure increases and the pump power needs to be increased too, to keep the same mass flow rate, which is realised by the experimental control. The increase in pump power causes an increase in mass flow rate, likely above the set-point value, and can brush aside the accumulated ice in front of the inlet resulting in a small free space around the inlet until it is covered by more ice particles. This process leads to a pulsing effect until complete blockage. The phases of "slightly blocked" vessel slurry inlet are therefore visible in the mass flow rate by fluctuations.

A "freeze alarm" was detected after almost 3 h and could be attributed to an ice formation in the supercooler itself (no complete blockage), likely caused by an ice particle entering the supercooler, and visible in the rise of the T_{WaOut} signal to 0 °C, mounted after the supercooler. By visual investigation it could be observed that ice particles moved into the former "ice-free" second storage due to the "full" ice slurry storage (see Fig. 7 C) from where they can be easily pumped to the supercooler. After finishing the test, a manual check of the ice consistency in the ice slurry storage revealed a lower packing density in top layers, which were filled in the beginning of the test-run, when ice crystals entering the storage were able to rise more freely. In comparison, the ice in lower layers, also around the inlet, was packed with a higher density and almost down to the bottom. However, the theoretically produced ice mass during this time with the used operational parameters is around 200 kg, occupying a volume of 0.23 m^3, which is 23 % of the complete slurry storage volume (one tank), making clear that the introduction of slurry into the vessel needs to be improved.

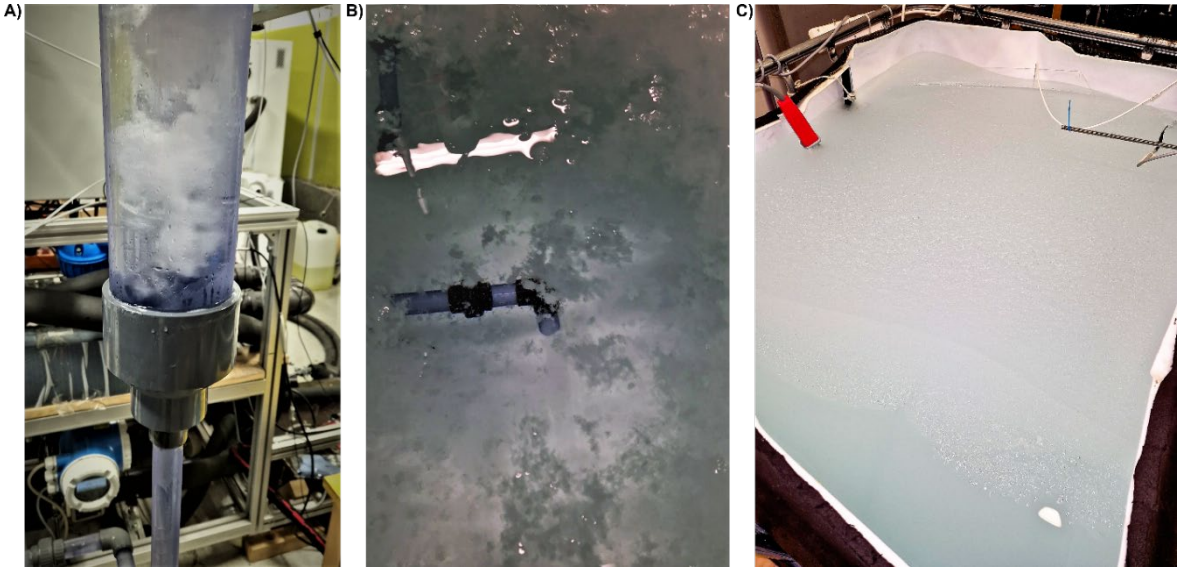

Figure 7: Photographs of A) the slurry generation inside the crystallizer, B) the produced slurry entering the storage vessel and C) the full storage vessel at the end of test-run as presented in Fig. 6.

4. Conclusion

This paper presents experimental developments and results for the reliable and continuous generation of ice slurry from an in-stream crystallizer using the supercooling method at a power of up to 6.5 kW.

The possibility to use gasketed plate heat exchangers reaching supercooling degrees suitable for ice slurry production between −1.5 °C and −2.5 °C without the need of icephobic coatings was shown. This possibility could decrease fabrication and installation cost of the technology as well as avoidance of coating degradation, decreasing thus maintenance needs. Gasketed plate heat exchangers are a suitable solution for large scale applications such as industrial processes. However, these type of heat exchangers are typically not suitable for residential heat pumps since they are too large. Moreover, the influence of the water quality is unclear at this stage as well as the question if icephobic coatings could provide a more stable system using tap water, likely with an increasing number of particles that could be expected after long term operation and that could trigger heterogeneous nucleation in the system. The effect of water quality on supercooling stability and the possible

increase of operation stability by using icephobic coatings, assuming a growing number of particles in the system with operation time, will be topic of further research in near future.

The development of the in-stream ice crystallizer, demonstrated at a mass flow rate of 3200 kg/h and an average supercooling degree of 1.75 K can become a breakthrough technology for energy storage paving the way to provide energy flexibility at low cost. However, to implement this technology at large scale, the scalability needs to be proven and optimisation needs to be conducted. To obtain more accurate and detailed insights into the in-stream crystallizer, further development of CFD modelling using multi-scale biphasic simulation is planned for near future, helping to realise the up-scaling of the crystallizer in an optimised configuration.

In this paper, two of the defined three challenges for the proposed ice slurry technology have been addressed and solutions for the supercooling and the continuous crystallisation have been presented. Nevertheless, the low maximum mass ice fraction achieved of approximately 23 % compared to the expected value of approximately 50 % (Kauffeld, et al., 2005) clearly shows that the third challenge remains to be investigated further. A better separation of solid particles and liquid water would allow to increase reliability as well as lowering the water inlet temperature into the supercooler to increase performance of the technology by reducing heat losses. Thus, the aforementioned third challenge of a proper separation of ice and water in the storage vessel needs to be content of future research work, before the proposed method is ready to be implemented into the field.

5. Acknowledgments

The authors thank the US Department of Energy (Solar Energy Technology Office) [Award Number DEEE0009814] and the Swiss Departement of Energy (SFOE) [Grant Number SI502570-01] for financial support.

We thank Alfred Brunner for support in the electrical and software control as well as Bruno Füchslin and Ramon Mattle for help in building the experimental set-up.

6. References

Arenas-Larranaga, M., Gurruchaga, I., Carbonell, D. & Martin-Escudero, K., 2024. Performance of solar-ice slurry systems for residential buildings in european climates. Energy and Buildings, Volume 307.

Bédécarrats, J.-P., David, T. & Castaing-Lasvignottes, J., 2010. Ice slurry production using supercooling phenomenon. International Journal of Refrigeration, 33(1), p. 196–204.

Carbonell, D. et al., 2020. Slurry-Hp II - Development of a supercooling ice slurry heat pump concept for solar heating applications, Bern: Institut für Solartechnik SPF for Swiss Federal Office of Energy (SFOE), Research Programme Heat Pumps and Refrigeration.

Carbonell, D., Philippen, D., Granzotto, M. & Haller, M. Y., 2016. Simulation of a solar-ice system for heating applications. System validation with one-year of monitoring data. Energy and Buildings, 127(0), p. 846 – 858.

Carbonell, D., Philippen, D., Haller, M. Y. & Frank, E., 2015. Modeling of an ice storage based on a de-icing concept for solar heating applications. Solar Energy, Volume 121, pp. 2-16.

Carbonell, D. et al., 2022. Development of supercoolers for ice slurry generators using icephobic coatings. Internationa Journal of Refrigeration, Volume 144, pp. 90-98.

Ernst, G. & Kauffeld, M., 2016. Influence of the wall surface roughness on the supercooling degree of water flowing inside a heat exchanger. Karlsruhe, Germany, International Journal of Refrigeration (IRR).

Faucheux, M., Muller, G., Havet, M. & LeBait, A., 2006. Influence of surface roughness on the supercooling degree : Case of selected water/ethanol solutions frozen on aluminium surfaces. International Journal of Refrigeration, Volume 29, p. 1218–1224.

Gurruchaga, I. et al., 2023a. Potential benefits of TRI-HP systems around Europe, s.l.: Deliverable 7.10 TRI-HP: Trigeneration systems based on heat pumps with natural refrigerants and multi renewable sources, Horizon 2020 research and innovation programme under grant agreement N. 814888.

Gurruchaga, I. et al., 2023b. Demonstrated energetic performance and cost competitiveness of tri-hp systems, s.l.: Deliverable 7.9 TRI-HP: Trigeneration systems based on heat pumps with natural refrigerants and multi renewable sources, Horizon 2020 research and innovation programme under grant agreement N. 814888.

Haberl, R. et al., 2022. Concise cycle test methods to evaluate heating/cooling systems with multiple renewable sources. s.l., CLIMA 2022 conference.

Honke, M., Safarik, M. & Herzog, R., 2015. R718 turbo chillers and vacuum ice generation - two applications of a new generation of high speed, high capacity R718 centrifugal compressors. s.l., 24th International Congress of Refrigeration.

Kauffeld, M. & Gund, S., 2019. Ice slurry − History, current technologies and future developments. International Journal of Refrigeration, Volume 99, p. 264–271.

Kauffeld, M., Kawaji, M. & Egolf, P., 2005. Handbooks on Ice Slurries: Fundamentals and Engineering. Paris: International Institute of Refrigeration (IIR).

Kozawa, Y., Aizawa, N. & Tanino, M., 2005. Study on ice storing characteristics in dynamic-type ice storage system by using supercooled water.: Effects of the supplying conditions of ice-slurry at deployment to district heating and cooling system. International journal of refrigeration, 28(1), pp. 73-82.

Kurihara, T. & Kawashima, M., 2001. Dynamic ice storage system using super cooled water. introductions of heat pump and thermal storage unit for commercial use. Osaka, Japan, Proceedings of the 4th Workshop on Ice Slurries of the IIR, pp. 61-69.

Lyons, L. et al., 2023. Clean energy technology observatory: Heat pumps in the european union - 2023 status report on technology development, trends, value chains and markets, s.l.: Publications Office of the European Union, Luxembourg.

Mito, D., Mikami, Y., Tanino, M. & Kozawa, Y., 2002. A New Ice Slurry Generator by Using Actively Thermal-hydraulic Controlling both Supercooling and Releasing of Water. s.l., Proceedings of the 5th Workshop on Ice Slurries of the IIR, pp. 185-196.

Mito, D., Tanino, M., Kozawa, Y. & Okamura, A., 2001. Application of a dynamic ice-type storage system to the intermittent cooling process in the food industry.

Mouneer, T. A., El-Morsi, M. S., Nosier, M. A. & Mahmoud, N. A., 2010. Heat transfer performance of a newly developed ice slurry generator: A comparative study. Ain Shams Engineering Journal, 1(2), pp. 147-157.

Nagato, H., 2001. A dynamic ice storage system with a closed ice-making device using supercooled water. Osaka, Japan, Proceedings of the 4th Workshop on Ice Slurries of the IIR, pp. 97-103.

Nelson, D. J., Vick, B. & Yu, X., 1996. Validation of the algorithm for ice-on-pipe brine thermal storage systems. ASHRAE Transactions, Volume 102, p. 55–62.

Philippen, D. et al., 2012. Development of a heat exchanger that can be de-iced for the use in ice stores in solar thermal heat pump systems. Rijeka and Opatija, International Solar Energy Society (ISES).

Pronk, P., Meewisse, J. M., Ferreira, C. A. I. & Witkamp, G. J., 2003. Ice slurry production with a circulating fluidized bed heat exchanger. Washington D.C., International Congress of Refrigeration.

Saito, A. & Okawa, S., 1994. Fundamental research on initiation of freezing of supercooled water on heat transfer surface. Brighton, United Kingdom, 10th International Heat Transfer Conference, p. 121–126.

Stamatiou, E., Meewisse, J. W. & Kawaji, M., 2005. Ice slurry generation involving moving parts. International Journal of Refrigeration, 28(1), pp. 60-72.

Tanino, M. & Kozawa, Y., 2001. Ice-water two-phase flow behavior in ice heat storage systems. International Journal of Refrigeration, 24(7), p. 639–651.

Tanino, M., Kozawa, Y., Mito, D. & Inada, T., 2000. Development of active control method for supercooling releasing of water. Proceedings of the 2nd Workshop on Ice Slurries of the IIR, Volume 127.

Wijeysundera, N. E., Hawlader, M. N. A., Andy, C. W. B. & Hossain, M. K., 2004. Ice-slurry production using direct contact heat transfer. International Journal of Refrigeration, 27(5), pp. 511-519.

Zhang, X. J. et al., 2008. Performance improvement of vertical ice slurry generator by using bubbling device. Energy Conversion and Management, 49(1), pp. 83-88.

Disclaimer